

Electronic Supplementary Information

Sn²⁺-Coordinated Polyethylenimine as Electron Transport Layer for High-Efficiency and Stable Inverted Organic Solar Cells

Yuntao Hu^{1†}, Shuo Wan^{1†}, Yi Li¹, Huiting Fu¹, Qingdong Zheng^{1*}

¹ State Key Laboratory of Coordination Chemistry, College of Engineering and Applied Sciences, Nanjing University, Nanjing 210023, China.

† These authors contributed equally to this work.

* Corresponding authors (email: zhengqd@nju.edu.cn).

Materials

PM6 and Y6 were purchased by Solarmer Materials Inc. Polyethylenimine (PEI, $M_w = 25,000$ g/mol), tin (II) acetate, cobalt (II) acetate, manganese (II) acetate, nickel (II) acetate, 1-butanol, 1-chloronaphthalene, chloroform, MoO_x were purchased from Sigma-Aldrich. All the other reagents and solvents were purchased commercially as analytically pure and used without further purification.

Device Fabrication

In this paper, OSCs were fabricated with an inverted structure of ITO/ETL/PM6:Y6/MoO_x/Ag. ITO glass was ultrasonically cleaned with detergent, deionized water, acetone and isopropanol for 15 min each, then dried overnight in an oven, and subsequently subjected to UV-O₃ treatment for 15 min prior to use. For the preparation of PEI ETL Solution, PEI (30 mg) was dissolved in 1.1 mL of 1-butanol and stirred at 80 °C for 12 h. The solution was then diluted to 0.01 wt% with 1-butanol. For the preparation of PEI-Sn²⁺ ETL Solution, PEI (30 mg) was dissolved in 1.1 mL of 1-butanol and stirred at 80 °C for 12 h. Then, different amount of tin (II) acetate was added into the PEI solution, and stirred for 3 h before coating. For the optimized Sn-to-N mole ratio of 3:1, 1.3 mg of tin (II) acetate was added to the 1 mL 0.01 wt% PEI

solution and stirred until the solution became clear. Afterward, The PEI, PEI-Sn²⁺ solutions were deposited on the cleaned ITO glass substrates by spin-coating at 3000 rpm for 30 s and the electron transport layer doesn't require annealing. The above operations are all done in the air environment. PM6 and Y6 were dissolved in chloroform solvent at a mass ratio of 1:1.2, the total concentration of the active layer solution was 16.5 mg/mL, and 0.6% volume of 1-chloronaphthalene was added, and stirred at 50 °C for 60 min. The BHJ active layer solution was spin-coated on top of the ETL layers at 3000 rpm for 30 s and thermally annealed at 80 °C/5 min. The above operations were all completed in the N₂ glove box. Finally, MoO_x (10 nm) and Ag (100 nm) were sequentially deposited on top of the BHJ active layer by thermal evaporation at 5×10^{-5} Pa through a shadow mask. The photoactive area of each BHJ unit was 0.042 cm².

Characterizations

X-ray photoelectron spectra (XPS) of Si/PEI and Si/PEI-Sn²⁺ were tested by the Thermo Scientific Al K-Alpha XPS system with energy steps of 0.1 eV. ¹H NMR spectra were measured on a Bruker Avance III 400 MHz spectrometer using deuterated methanol and deuterated Chloroform as the solvent with tetramethylsilane ($\delta=0$) as the internal standard. The absorption and transmittance spectra were measured by a UV-vis spectrophotometer (UV-2600i). Ultraviolet photo-electron spectroscopy (UPS) was tested by Thermo Fisher Scientific Nexsa with using a He I discharge lamp. Atomic force microscopy (AFM) of the ITO/PEI and ITO/PEI-Sn²⁺ sample were measured through tapping mode with a Bruker Dimension Icon instrument in air. The water and diiodomethane contact angle images of neat films were recorded by using a CA100C under atmospheric conditions. The conductivity of ETLs is estimated by measuring the current-voltage (*I-V*) curves of the devices with the sandwich structure ITO/ETL/Ag based on Ohm's law. Current density-voltage (*J-V*) characteristics were recorded in the glove box with a Keithley 2400 Source Measure Unit under room temperature. The photocurrent was tested under AM 1.5G illumination at 100 mW cm⁻² using a solar simulator (SS-X50, Enlitech). The EQE spectra were measured by using a solar-cell

spectral-response measurement system (QE-R, Enlitech). The electrochemical impedance spectroscopy (EIS) measurements were characterized by the CHI604E electrochemical workstation, at frequencies from 1 MHz to 10 Hz. A bias voltage equal to V_{oc} was applied to offset the total current.

Photocurrent density (J_{ph})-effective voltage (V_{eff}) measurements.

The photocurrent density J_{ph} is defined as $J_{ph} = J_L - J_D$, where J_L and J_D are the photocurrent densities under illumination and in the dark, respectively. The effective voltage V_{eff} is defined as $V_{eff} = V_0 - V_{bias}$, where V_0 is the voltage at which J_{ph} is zero and V_{bias} is the applied external voltage bias. The V_{eff} raises a suitable internal electric field in the device to suppress the charge recombination. In our case, the J_{ph} is saturated at V_{eff} of 1 V. The charge dissociation probability (P_{diss}) was estimated by the value of J_{ph}/J_{sat} , where J_{sat} represents the saturated photocurrent density.

Hole- and Electron-Only Device Fabrication and Characterization

Hole and electron mobilities were measured using the space charge limited current (SCLC) method. Hole-only devices were fabricated with ITO/PEDOT:PSS/PM6:Y6/MoO_x/Ag, while electron-only devices were fabricated with ITO/ETL/ PM6:Y6/PNDIT-F₃N/ Ag. The active layers were prepared using the same method for the best-performance OSC fabrication. Device areas were fixed at 0.042 cm². A Keithley 2440 source measurement unit measured the current density (J). The SCLC hole/electron mobilities were calculated according to the following equation:

$$J = \frac{9\epsilon_r\epsilon_0\mu V^2}{8L^3}$$

Where J is the current density (A m⁻²), ϵ_0 is the free-space permittivity (8.85×10^{-12} F m⁻¹), and ϵ_r is the relative dielectric constant of the active layer material, usually 2-4 for organic semiconductors, herein we used a relative dielectric constant of 3, μ is the mobility of hole or electron, V is the voltage drop across the SCLC device ($V = V_{app} - V_{bi}$, where V_{app} is the applied voltage to the device and V_{bi} is the built-in voltage due to the difference in the work function of two electrodes, in the hole- and electron-only devices,

the V_{bi} values are 0.5 and 0.7 V, respectively), and L is the thickness of the active layer. The film thickness was detected by a Bruker Dektak XT surface profilometer. The hole- or electron mobilities were calculated from the slopes of the $J^{1/2}$ - V curves.

Stability Measurements

Storage Stability:

Unencapsulated devices were placed in an N_2 -filled glove-box.

Thermal stability:

For thermal stability evaluation, unencapsulated devices were heated at 65 °C on a hotplate under the open-circuit conditions in an N_2 -filled glove-box.

Photostability:

The stability tracked under continuous illumination (100 mW cm^{-2}) at maximum power point (MPP) was investigated based on optimum devices.

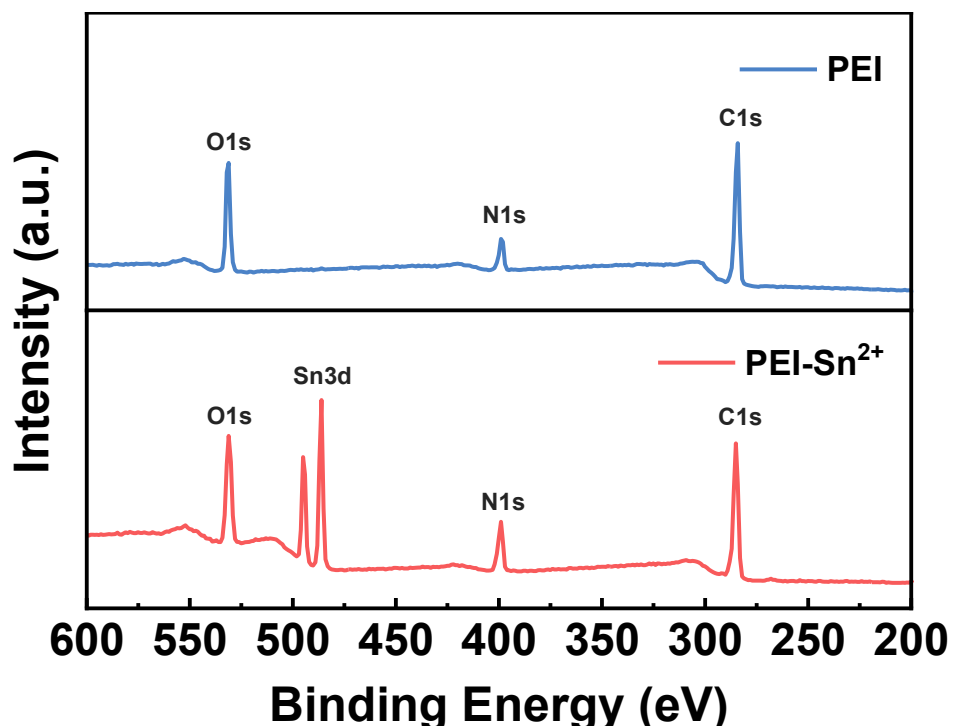


Figure S1. The full XPS spectra of PEI and PEI- Sn^{2+} .

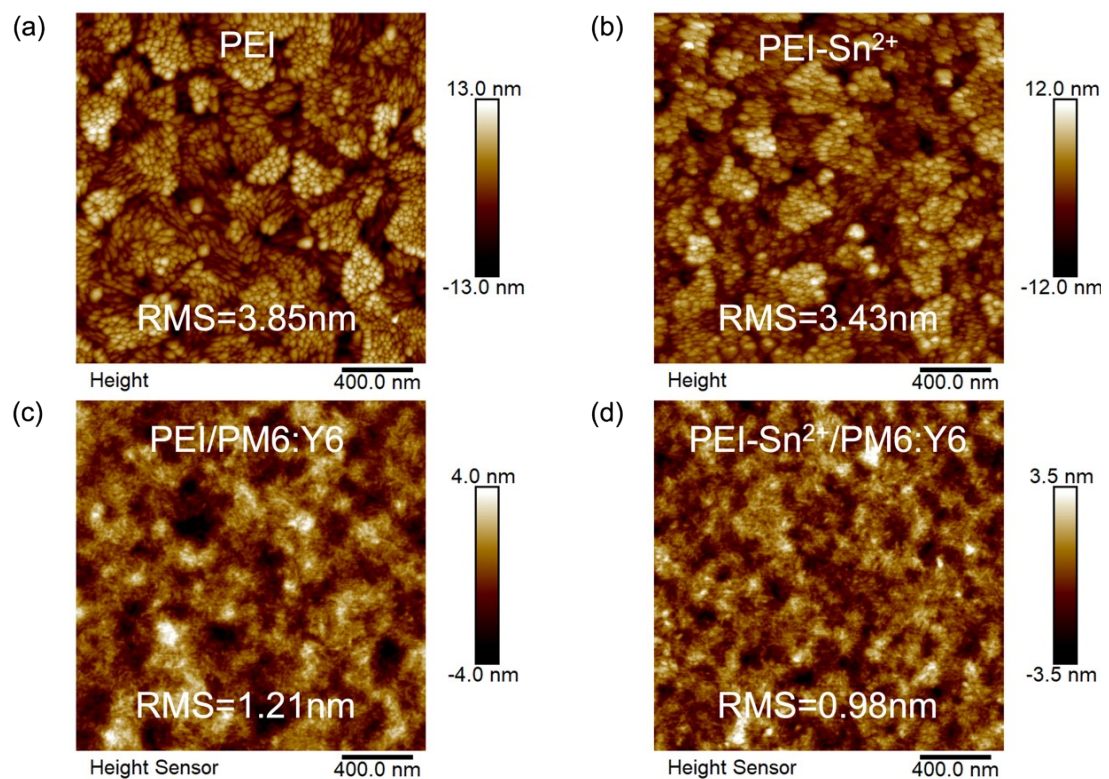


Figure S2. AFM height images of a) PEI, b) PEI-Sn²⁺, c) PEI/PM6:Y6, d) PEI-Sn²⁺/PM6:Y6.

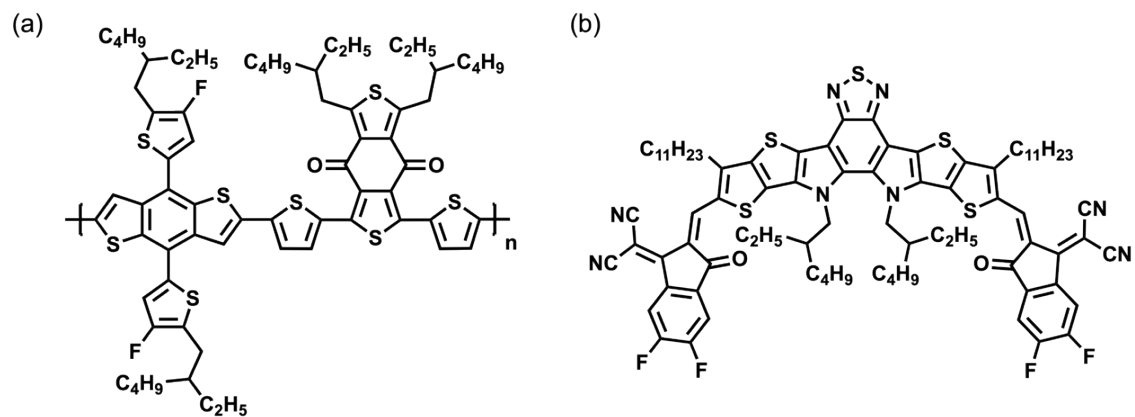


Figure S3. The chemical structures of a) PM6 and b) Y6 used in the devices.

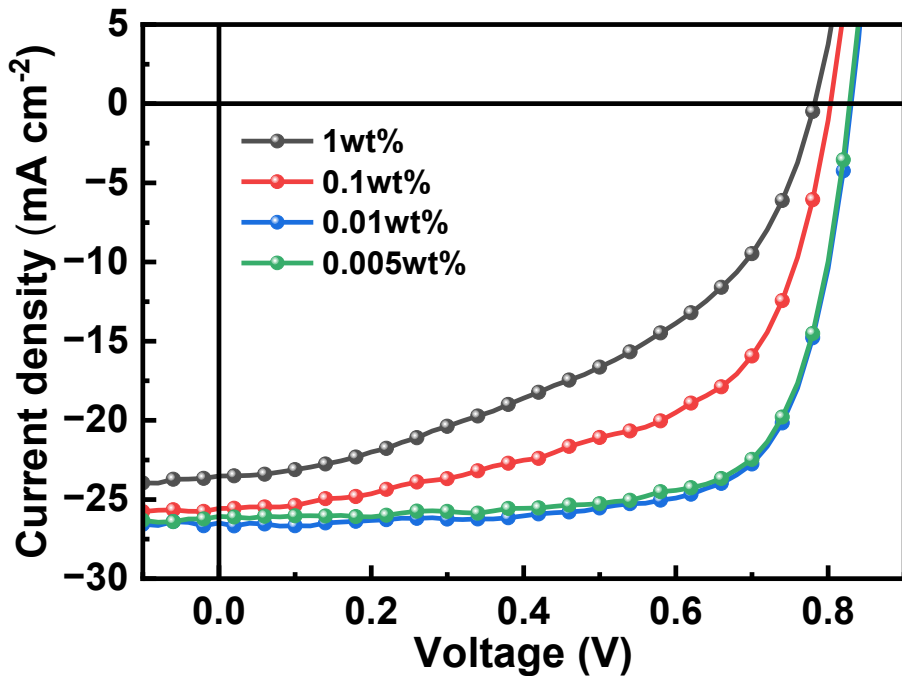


Figure S4. J - V characteristics of PM6:Y6 devices based on PEI ETL of different thicknesses.

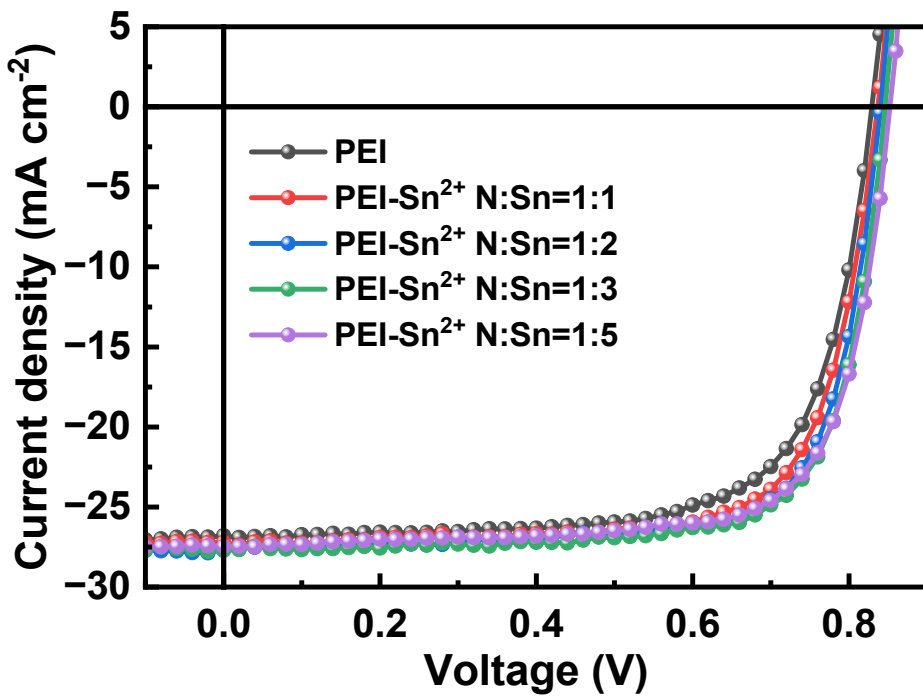


Figure S5. J - V characteristics of PM6:Y6 devices with PEI-Sn $^{2+}$ ETL containing different N-to-Sn mole ratios.

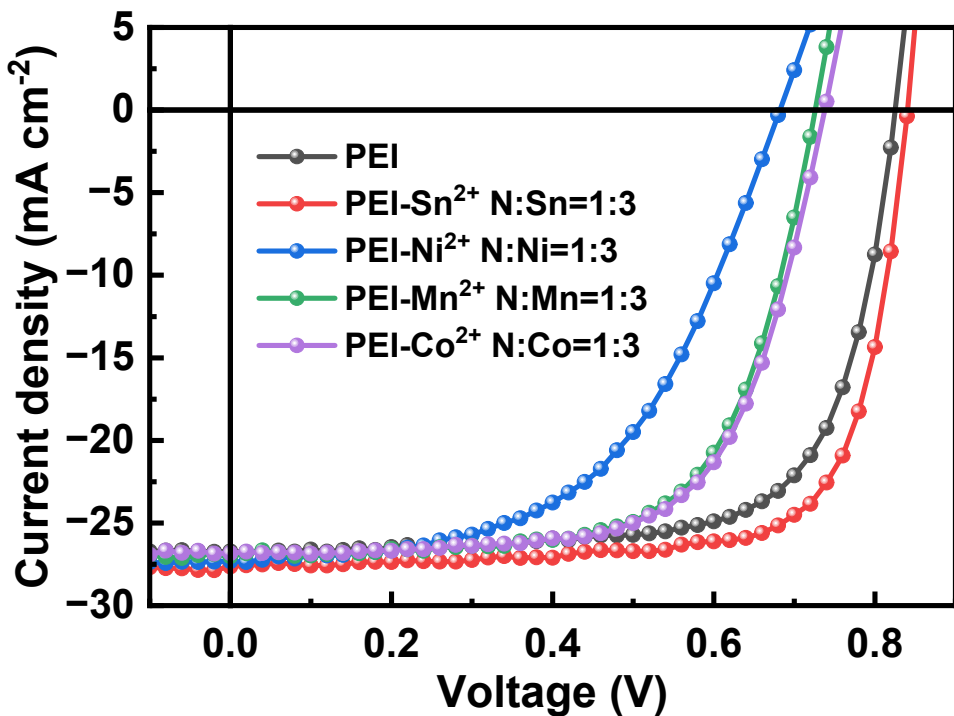


Figure S6. J - V characteristics of PM6:Y6 devices with different ions coordinated PEI ETLs.

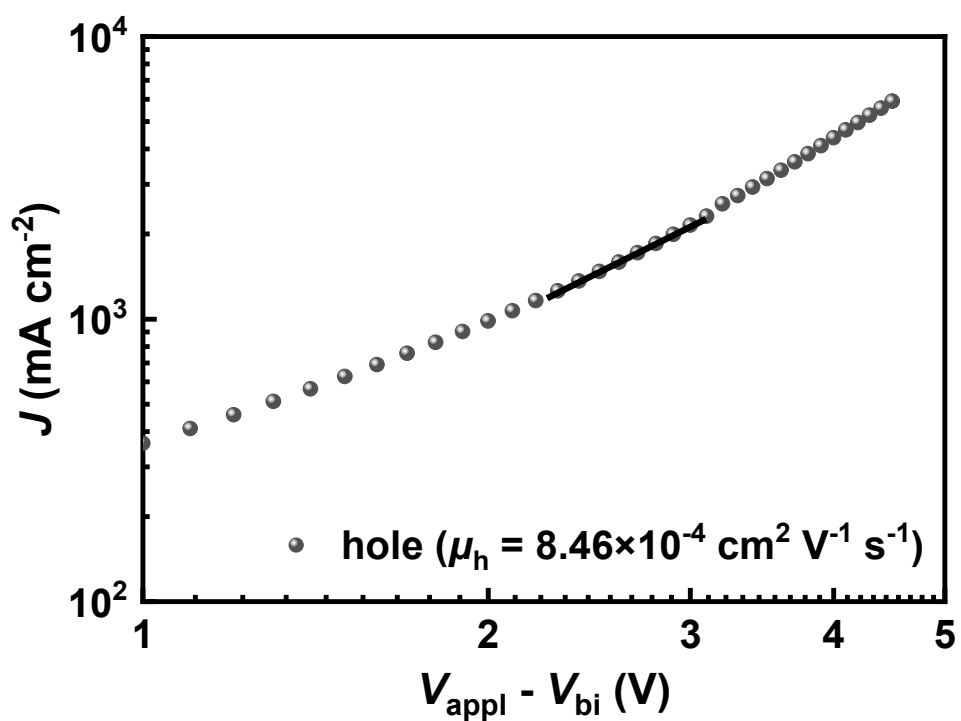


Figure S7. SCLC curve for the hole-only device based on PM6:Y6.

Table S1. Contact angles, surface tensions γ

Surface	θ_{Water} [deg]	$\theta_{\text{Diiodomethane}}$ [deg]	γ [mN m ⁻¹]
ITO	33.4	33.5	63.1
ITO/PEI	31.2	22.4	65.7
ITO/PEI-Sn ²⁺	46.8	49.4	52.8
PM6:Y6	99.1	51.0	34.3

The surface tension was calculated by

$$\gamma_{\text{water}}(1 + \cos \theta_{\text{water}}) = 2\sqrt{\gamma_{\text{water}}^d \gamma^d} + 2\sqrt{\gamma_{\text{water}}^p \gamma^p}$$

$$\gamma_{\text{DI}}(1 + \cos \theta_{\text{DI}}) = 2\sqrt{\gamma_{\text{DI}}^d \gamma^d} + 2\sqrt{\gamma_{\text{DI}}^p \gamma^p}$$

$$\gamma_{\text{total}} = \gamma^d + \gamma^p$$

where θ is the droplet contact angle on the organic thin film; γ_{total} is the surface tension of the organic material, which is equal to the sum of the dispersion (γ^d) and polarity (γ^p) components; γ_i is the surface tension of the liquid droplet (water or DI); γ^d and γ^p are the dispersion and polarity components of γ_{total} , respectively.

Table S2. Photovoltaic Parameters of PM6:Y6 devices based on PEI ETL of different thicknesses under the illumination of AM 1.5 G, 100 mW cm⁻²

PEI ETL	V_{oc} (V)	J_{sc} (mA cm ⁻²)	FF (%)	PCE (%)
1 wt%	0.782	23.6	45.9	8.43
0.1 wt%	0.804	25.6	57.4	11.8
0.01 wt%	0.826	26.6	72.2	15.8
0.005 wt%	0.822	26.4	71.6	15.7

Table S3. Photovoltaic parameters of PM6:Y6 devices with PEI-Sn²⁺ ETL containing different N-to-Sn mole ratios under the illumination of AM 1.5 G, 100 mW cm⁻²

ETL	V_{oc} (V)	J_{sc} (mA cm ⁻²)	FF (%)	PCE (%)
PEI	0.827	26.9	70.9	15.7
PEI-Sn ²⁺ N:Sn=1:1	0.835	27.3	73.1	16.7
PEI-Sn ²⁺ N:Sn=1:2	0.839	27.7	73.9	17.3
PEI-Sn ²⁺ N:Sn=1:3	0.845	27.7	74.4	17.5
PEI-Sn ²⁺ N:Sn=1:5	0.850	27.5	73.5	17.2

Table S4. Photovoltaic parameters of PM6:Y6 devices with different ions coordinated PEI ETLs under the illumination of AM 1.5 G, 100 mW cm⁻²

ETL	V_{oc} (V)	J_{sc} (mA cm ⁻²)	FF (%)	PCE (%)
PEI	0.824	26.7	70.9	15.6
PEI-Sn ²⁺ N:Sn=1:3	0.840	27.7	74.2	17.3
PEI-Ni ²⁺ N:Ni=1:3	0.682	27.3	53.3	9.9
PEI-Mn ²⁺ N:Mn=1:3	0.725	26.9	65.9	12.8
PEI-Co ²⁺ N:Co=1:3	0.737	26.8	66.1	13.0

Table S5. Charge-transporting properties of the PEI and PEI-Sn²⁺ based devices

ETL	μ_e (10 ⁻⁴ cm ² V ⁻¹ s ⁻¹) ^{a)}	μ_e/μ_h
PEI	7.30 (7.07 ± 0.36)	0.86
PEI-Sn ²⁺	9.01 (8.78 ± 0.30)	1.06

^{a)} In parentheses are average values with standard deviations based on 5 devices.

Table S6. Comparison of the PCE in this work with those of the inverted OSCs in some recent reports

Active layer	ETL	PCE (%)	Ref.
PBDB-T-2F:IT-4F	PEI-Zn	13.29	S1
PM6:Y6:PC ₇₁ BM	ZnO/a-PEI	15.70	S2
PM6:Y6	PEI-Ph	16.34	S3
PM6:Y6:PC ₇₁ BM	carbon dots	16.80	S4
PM6:BTP-BO-4F:PC ₇₁ BM	PEI-GDE-BS	17.55	S5
PM6:Y6	ZnO-P	16.47	S6
PM6:Y6	PDIEIE	15.04	S7
PM6:Y6	PEI-Sn ²⁺	17.50	This work

References

- S1. F. Qin, W. Wang, L. Sun, X. Jiang, L. Hu, S. Xiong, T. Liu, X. Dong, J. Li, Y. Jiang, J. Hou, K. Fukuda, T. Someya and Y. Zhou, *Nat. Commun.*, 2020, **11**, 4508.
- S2. L. Hu, Y. Y. Jiang, L. L. Sun, C. Xie, F. Qin, W. Wang and Y. H. Zhou, *J. Phys. Chem. Lett.*, 2021, **12**, 2607-2614.
- S3. L. Hu, W. You, C. Xie, H. Zheng, L. Han, D. Zhou, Y. Jin, J. Song, X. Yin, Z. Su, Y. Zhou and Z. Li, *Sol. RRL*, 2022, **6**, 2200486.
- S4. Y. Dong, R. Yu, B. Zhao, Y. Gong, H. Jia, Z. Ma, H. Gao and Z. A. Tan, *ACS Appl. Mater. Interfaces*, 2022, **14**, 1280-1289.
- S5. H. Nie, M. Busireddy, H. Shih, C. Ko, J. Chen, C. Chang and C. Hsu, *ACS Appl. Mater. Interfaces*, 2023, **15**, 1718-1725.
- S6. H. Zheng, D. Zhou, L. Hu, Z. Xu, H. Xu, Y. Zhang, Y. Tong, B. Hu, Z. Li and L. Chen, *Sol. RRL*, 2022, **6**, 2200871.
- S7. Y. Li, T. Li, J. Wang, X. Zhan and Y. Lin, *Sci. Bull.*, 2022, **67**, 171-177.